Formation of Si nanocrystallites observed by in situ transmission electron microscopy and their effect on the enhancement of Er photoluminescence in Er-doped SiO2

doi: 10.1063/1.2817639

Formation of Si nanocrystallites observed by *in situ* transmission electron microscopy and their effect on the enhancement of Er photoluminescence in Er-doped SiO_2

N. Fukata[a),b),c)]
Advanced Electronic Materials Center, National Institute for Materials Science, 1-1 Namiki, Tsukuba 305-0044, Japan

H. Morihiro, R. Shirakawa, and K. Murakami[b)]
Institute of Applied Physics, University of Tsukuba, Tsukuba 305-8573, Japan

M. Mitome and Y. Bando
Nanoscale Materials Center, National Institute for Materials Science, 1-1 Namiki, Tsukuba 305-0044, Japan

(Received 15 August 2007; accepted 1 October 2007; published online 12 December 2007)

The formation of Si nanocrystallites (nc-Si) in erbium (Er)-dispersed SiO_x ($x \leqslant 2$) films was investigated by *in situ* annealing while performing transmission electron microscopy measurements. The correlation between the formation of nc-Si and Er ion emissions was also comprehensively investigated by photoluminescence and electron spin resonance measurements. The results showed that the formation of nano-Si region with the suitable size is important for enhancement of Er ion emission. © *2007 American Institute of Physics*. [DOI: 10.1063/1.2817639]

I. INTRODUCTION

The sensitization of Er ion emission ($\lambda = 1.54\ \mu m$) by host materials, such as crystalline Si (*c*-Si),[1,2] amorphous Si (*a*-Si),[3,4] and Si nanocrystallites (nc-Si),[5–15] has been extensively investigated. In the case of *c*-Si, the nonradiative deexcitation process leads to thermal quenching of Er ion emission.[2] The second *a*-Si case shows a weaker temperature dependence of Er ion emission than in the *c*-Si case; however, lifetime is a problem.[3,4] On the other hand, the effective excitation cross section of nc-Si is much higher than that of resonant excitation for Er ion in SiO_2,[12,13] and the decay time of the Er ion emission is close to being temperature independent.[11,13] Hence, nc-Si is regarded as one of the most promising sensitizers. More recently, we have synthesized Er-doped SiO_2 including nc-Si by laser ablation and investigated the hydrogen passivation effect of interfacial defects between nc-Si and the SiO_2 matrix in enhancing energy transfer from nc-Si to Er ions, resulting in enhanced Er ion emission.[16]

To maximize the effectiveness of nc-Si, it is necessary to further investigate the formation process of nc-Si within an SiO_2 matrix. In the present study, we investigated this by *in situ* annealing while taking transmission electron microscopy (TEM) measurements and *ex situ* annealing in an electronic furnace. The correlation between the formation of nc-Si and the Er ion was also comprehensively investigated by photoluminescence (PL) and electron spin resonance (ESR) measurements. The results showed the size and density of nc-Si to be important for the enhancement of Er ion emission.

II. EXPERIMENT

Erbium-dispersed SiO_x ($x \leqslant 2$) films containing nc-Si were prepared by laser ablation: Er thin films were deposited on Si substrates in a vacuum by ablating Er metal plates, after which the Si substrates with Er thin films were laser ablated in O_2 gas at a pressure of 40 mTorr to deposit Er-dispersed SiO_x films. The laser light used was a 532 nm Nd:YAG (YAG denotes yttrium aluminum garnet) laser light with a pulse duration of 7 ns and a fluence of about 4 J/cm^2. After the pulsed laser deposition, *in situ* annealing was performed to directly investigate the formation process of nc-Si in the Er-dispersed SiO_x films. This *in situ* annealing was performed using a TEM grid holder with a heater. After the specimens had been annealed for about 30 min at each temperature, TEM images were taken at four areas (an area: $40 \times 40\ \mu m^2$). These procedures were repeated from 200 to 900 °C. To observe the effect of heating by electron beam irradiation during the TEM observations, some of the Er-dispersed SiO_x films were annealed in an electronic furnace under an Ar gas flow for 30 min at 400–900 °C. The Er concentration was estimated to be about $2 \times 10^{20}\ cm^{-3}$ by Rutherford backscattering spectroscopy using 1.5 MeV protons at a backscattering angle of 150°. The mean Si and O compositions of the film were also estimated to be about 40 and 60 at. %, respectively.

III. RESULTS AND DISCUSSION

PL spectra of Er ions and nc-Si were detected using an InGaAs detector employing a lock-in amplifier system and Si photodiode, respectively, at RT. The excitation source was a

[a)]Present address: International Center for Materials Nanoarchitectonics, National Institute for Materials Science, 1-1 Namiki, Tsukuba, 305-0044, Japan.
[b)]Also at PRESTO, Japan Science and Technology Agency, 4-1-8 Honcho Kawaguchi, Saitama 332-0012, Japan. Electronic mail: FUKATA.Naoki@nims.go.jp.
[c)]Also at Special Research Project on Nanoscience, University of Tsukuba, Tsukuba 305-8573, Japan.

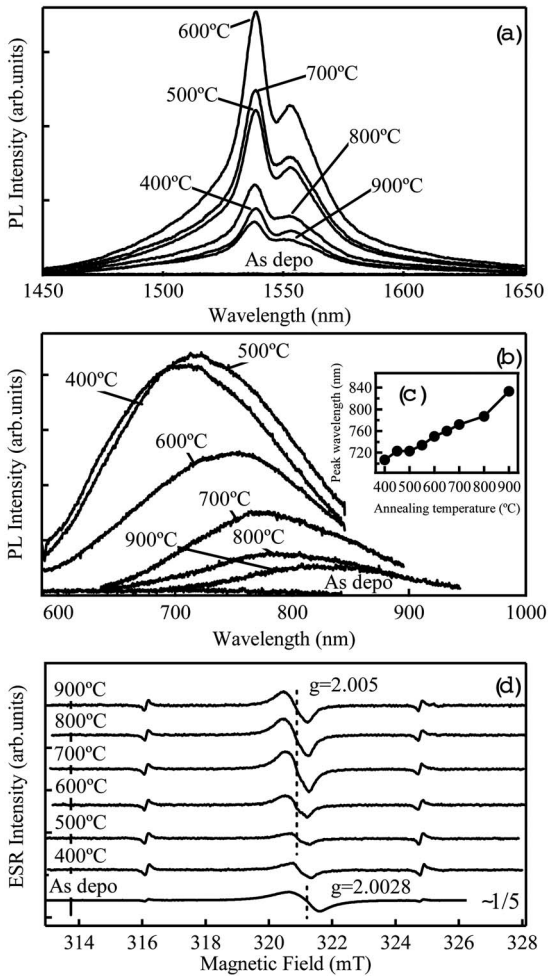

FIG. 1. Annealing temperature dependence of (a) Er PL and (b) nano-Si PL and (d) of the ESR signal of residual defects. The inset (c) shows the annealing temperature dependence of the peak position of nano-Si PL. These annealings were performed in Ar gas.

cw He–Cd laser light at 325 nm. ESR measurements were carried out at RT using an *X*-band ESR spectrometer. The derivative of resonant microwave absorption with respect to the magnetic field was measured using a lock-in amplifier and magnetic field modulation with a frequency of 100 kHz. The microwave power was set at 1 mW. An external ESR standard signal of Mn^{2+} in MgO was used to take into account possible changes in the quality factor of the microwave resonator among separate measurements. TEM (JEOL, JEM-3100FEF) measurements at various temperatures were performed to make direct observations of the formation of nc-Si in the SiO_2 films.

Figures 1(a) and 1(b) show the *ex situ* annealing temperature dependence of the PL spectra observed in two regions, and Fig. 1(d) that of the ESR signal of defects in an Er-dispersed SiO_x film. This annealing was performed in a furnace to investigate the formation of nc-Si in Er-dispersed SiO_x films. Before the *ex situ* annealing, no PL spectra of Er ions or nc-Si were observed, indicating that nc-Si was not included in the film and the film was defective. Figure 1(a) shows the PL spectrum of Er ions with increasing annealing temperature. A broad PL spectrum was also observed at around 700 nm after annealing at 400 °C; the peak showed a redshift with increasing annealing temperature, as shown in Fig. 1(b). The results are summarized in Fig. 1(c). The broad PL spectra are probably due to PL from nc-Si or amorphous Si nanograins composed of few Si atoms.[17] The assignments will be explained later based on the TEM results. Hereinafter, we call these broad PL spectra nano-Si PL. The redshift can be explained by the decrease in the band gap of Si nanostructures due to the increase in the size of nc-Si or the transformation of amorphous Si nanograins to nc-Si. The intensity of the broad PL showed a maximum for the specimen annealed at 500 °C. On the other hand, the PL intensity of Er ion peaked at 600 °C.

The ESR signals in Fig. 1(d) are due to defects in the Er-dispersed SiO_x films. Before *ex situ* annealing, the *g* value of the ESR signal was about 2.0028. The ESR signals showed a shift to a lower magnetic field with increasing annealing temperature, finally reaching a position with a *g* value of 2.005. The *g* values of oxygen-deficient defects ($Si_{3-x}O_x \equiv Si\cdot$; $x=1-3$) in SiO_x are in the range of 2.002–2.004, depending on the structures, i.e., *g* values increase on decreasing the number of oxygen atoms. With increasing annealing temperature, the SiO_x film is transformed into perfect SiO_2, resulting in the precipitation of nc-Si. Finally, defects are present only in the interface between the SiO_2 matrix and nc-Si. This defect is a kind of interfacial defect, a so-called P_b center ($Si_3 \equiv Si\cdot$). The ESR signals with *g* value of 2.002–2.004 are thus probably due to oxygen-deficient defects in the SiO_x film and that of 2.005 due to P_b centers. The intensity of the ESR signal increased with increasing annealing temperature. It also indicates that the formation of nc-Si proceeds with increasing annealing temperature.

TEM measurements were performed for specimens annealed in the furnace at 500, 700, and 900 °C. The *ex situ* annealing at 500 and 700 °C showed no nc-Si formation, while the results of PL in Fig. 1(b) show the maximum intensity after *ex situ* annealing at 500 °C. These results suggest that the annealing temperatures at 500 and 700 °C are not sufficiently high for the formation of nc-Si or that the size of nc-Si is below 1 nm, since the detection limit of nc-Si is around 1 nm in our TEM system. In the case of the latter, nc-Si with diameters below 1 nm is considered as the origin of the nano-Si PL, while in the former case, amorphous Si nanograins[17] may be the origin of the PL. On the other hand, nc-Si with diameters ranging from 3 to 5 nm were observed in the specimen after the *ex situ* annealing at 900 °C.[16] The diameter distribution of nc-Si after *ex situ* annealing is shown in Fig. 3. The result is explained later in addition to results of *in situ* annealing.

To further investigate the formation process of nc-Si in the Er-dispersed SiO_x film over a wide temperature range, *in situ* annealing was performed during TEM observations. Typical TEM images are shown in Fig. 2. The dependences of the diameter and the density of nc-Si on the annealing temperature are summarized in Fig. 3. The data in Figs. 3(a)–3(f) correspond to *in situ* annealing cases, while those in Figs. 3(g) and 3(h) correspond to *ex situ* annealing cases. Here, the counts in the vertical axis in Fig. 3 indicate the number of nc-Si observed in a region of 6400 μm^2. The lattice fringes of Si crystal were clearly observed in the films

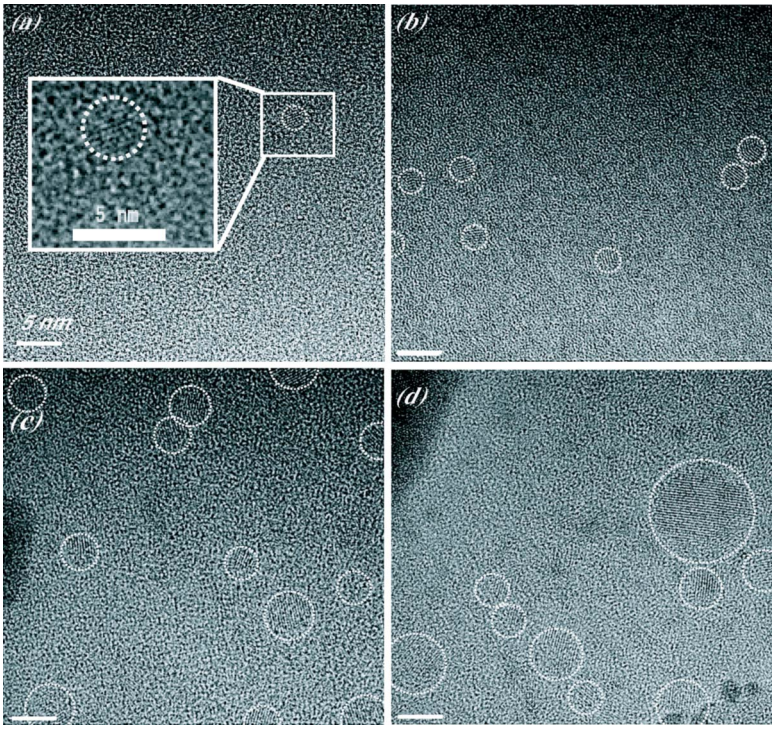

FIG. 2. (Color online) TEM micrographs of Er-dispersed SiO_x ($x \leqslant 2$) films annealed at (a) 400, (b) 500, (c) 700, and (d) 900 °C during TEM observations. The nc-Si regions are marked by dotted circles.

marked by dotted circles after *in situ* annealing at 400–900 °C. The diameter of nc-Si was about 3 nm after *in situ* annealing at 400 °C and it reached about 10 nm after *in situ* annealing at 900 °C. These results clearly show that the diameter and the density of nc-Si increase with increasing annealing temperature.

The formation temperatures of nc-Si shown in Fig. 2 are significantly different from those for the specimens annealed in the furnace. The formation of nc-Si could not be observed, even for the specimen after *ex situ* annealing at 700 °C, as shown in Fig. 3(g). Electron beam-assisted annealing during TEM observations is the one of the reasons, since electron beam irradiation increases the local temperature of the irradiated part of the specimen depending on the electron beam current. Considering the beam current density, the temperature rise is probably less than 300 °C, indicating that another additional effect has to be considered, since the formation of nc-Si was observed from 400 °C in the case of *in situ* annealing, but not even for the specimen after *ex situ* annealing at 700 °C in the furnace. Electron-nuclear collision by electron beam irradiation may be a factor. It often induces defects, resulting in atomic displacement by the subsequent diffusion of defects. This probably promotes the precipitation of amorphous Si nanograins and finally their crystallization. The role of the electron beam-assisted annealing is to increase the temperature in the irradiated part of the specimen and to cause the precipitation of nc-Si, while that of the electron-nuclear collision causes the further enhancement of the precipitation of nc-Si by using defects introduced. The result of *ex situ* annealing at 900 °C in Fig. 3(h) shows the similar tendency to that for the case of *in situ* annealing at 500–600 °C in Figs. 3(a)–3(c). However, the density of nc-Si for the *ex situ* annealing case is lower than that for the *in situ* annealing cases. Considering these results, we think that the electron-nuclear collision corresponds to the tem-

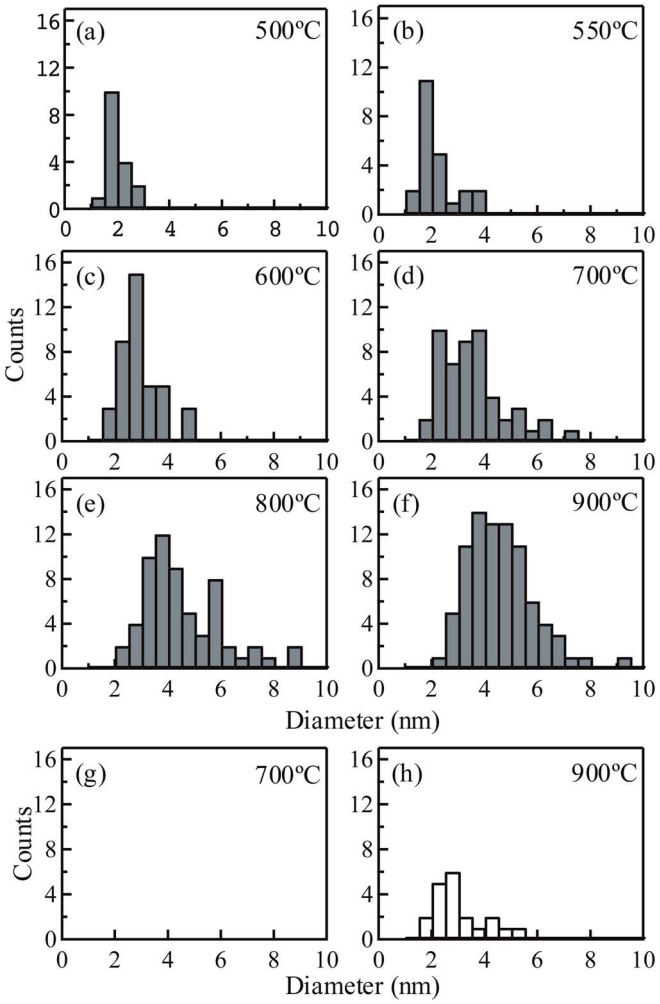

FIG. 3. (Color online) Histograms of diameter distribution of nc-Si formed in Er-dispersed SiO_x ($x \leqslant 2$) films by *in situ* annealing at (a) 500, (b) 600, (c) 700, (d) 800, and (e) 900 °C and *ex situ* annealing at (f) 700 and (g) 900 °C.

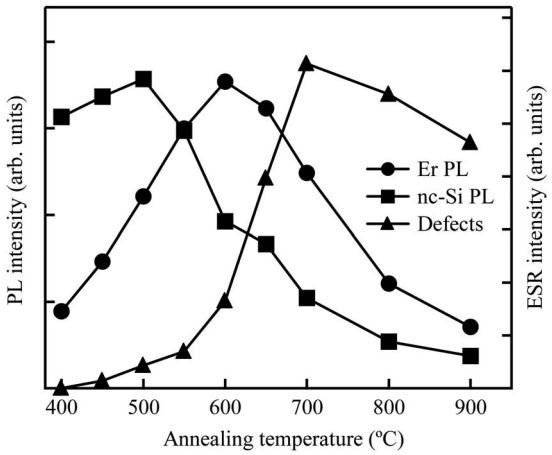

FIG. 4. Annealing temperature dependence of the PL intensities of Er ions and nano-Si, and of the ESR intensity of residual defects.

perature rise of about 100 °C. We also investigated the effect on temperature during electron beam irradiation. A sample was annealed at 700 °C for 30 min in TEM chamber without electron beam irradiation and then investigated by TEM at RT. No trace of crystallization was observed by TEM at RT. This result indicates that irradiation temperature is important for the formation of nc-Si, namely, the electronic and collisional effects by the electron beam are thermally activated.

Figure 4 shows a summary of the results of Fig. 1, namely, the results of *ex situ* annealing. There is a clear inverse correlation between the intensity of nano-Si PL and that of the ESR defect signal. This means that the interfacial defects formed between nano-Si and the surrounding SiO_x matrix act as nonradiative defects. The decrease in the intensity of nano-Si PL can thus be mainly explained by the increase in the size of nc-Si, and thereby the formation of interfacial defects. There is another reason for the decrease in the intensity of nano-Si PL, namely, the energy transfer from nano-Si to Er ions. In fact, an inverse correlation between Er PL and nano-Si PL was also observed in the region of 500–600 °C, indicating that excited nano-Si transfer energy to Er ions. Based on these, the increase in the Er PL intensity is due to the formation of nano-Si of suitable size and thereby an increase in energy transfer from nano-Si. On the other hand, the decrease is due to the decrease in energy transfer from nano-Si to Er ions, which is caused by the increase in the size of nano-Si and the formation of interfacial defects. The remaining problem concerns the suitable size of nano-Si. As already described, no formation of nc-Si was observed in the specimen annealed at below 700 °C. This result shows that nc-Si with a diameter less than 1 nm or amorphous Si nanograins are effective for enhancing Er PL.

IV. CONCLUSION

The formation of nc-Si in Er-dispersed SiO_x ($x \leqslant 2$) films was investigated by performing TEM measurements during *in situ* annealing. The correlation between the formation of nc-Si and Er ion emission was also comprehensively investigated by PL and ESR measurements. The results show that the formation of nano-Si region with the suitable size is important for the enhancement of Er ion emission.

ACKNOWLEDGMENTS

TEM observations were partly supported by the Nanotechnology Support Project of the Ministry of Education, Culture, Sports, Science and Technology (MEXT), Japan.

[1] S. Coffa, F. Priolo, G. Franzo, V. Bellani, A. Carnera, and C. Spinclla, Phys. Rev. B **48**, 11782 (1993).
[2] F. Priolo, G. Franzò, S. Coffa, A. Polman, S. Libertino, R. Barklie, and D. Carey, J. Appl. Phys. **78**, 3874 (1995).
[3] W. Fuhs, I. Ulber, G. Weiser, M. S. Bresler, O. B. Gusev, A. N. Kuznetsov, V. Kh. Kudoyarova, E. I. Terukov, and I. N. Yassievich, Phys. Rev. B **56**, 9545 (1997).
[4] H. Kuhne, G. Weiser, E. I. Terukov, A. N. Kuznetsov, and V. Kh. Kudoyarova, J. Appl. Phys. **86**, 896 (1999).
[5] J. H. Shin, G. N. van den Hoven, and A. Polman, Appl. Phys. Lett. **66**, 2379 (1995).
[6] U. Hommerich, F. Namavar, A. Cremins, and K. L. Bray, Appl. Phys. Lett. **68**, 1951 (1996).
[7] M. Fujii, M. Yoshida, S. Hayashi, and K. Yamamoto, J. Appl. Phys. **84**, 4525 (1998).
[8] S. Seo and J. H. Shin, Appl. Phys. Lett. **75**, 4070 (1999).
[9] G. Franzo, V. Vinciguerra, and F. Priolo, Appl. Phys. A **A69**, 3 (1999).
[10] M. L. Brongersma, P. G. Kik, A. Polman, K. S. Min, and H. A. Atwater, Appl. Phys. Lett. **76**, 351 (2000).
[11] P. G. Kik, M. L. Brongersma, and A. Polman, Appl. Phys. Lett. **76**, 2325 (2000).
[12] F. Priolo, G. Franzò, D. Pacifici, V. Vinciguerra, F. Iacona, and A. Irrera, J. Appl. Phys. **89**, 264 (2001).
[13] A. J. Kenyon, C. E. Chryssou, C. W. Pitt, T. S. Iwayama, D. E. Hole, N. Sharma, and C. J. Humphreys, J. Appl. Phys. **91**, 367 (2002).
[14] C. Li, K. Kondo, T. Makimura, and K. Murakami, Jpn. J. Appl. Phys., Part 1 **42**, 3424 (2003).
[15] T. Makimura, K. Kondo, H. Uematsu, C. Li, and K. Murakami, Appl. Phys. Lett. **83**, 5422 (2003).
[16] N. Fukata, C. Li, H. Morihiro, M. Mitome, Y. Bando, and K. Murakami, Appl. Phys. A: Mater. Sci. Process. **84**, 395 (2006).
[17] F. Enrichi, G. Mattei, C. Sada, E. Trave, D. Pacifici, G. Franzo, F. Priolo, F. Iacona, M. Prassas, M. Falconieri, and E. Borsella, Opt. Mater. (Amsterdam, Neth.) **27**, 904 (2005).